

Machine Learning-Based Dynamic Performance Prediction and Structural Parameter Optimization of a Two-Stage Hydrogen Pressure Reducing Valve



Huaxing Zhai^{3*}, Yu Zhang^{1,2}, Shuxun Li^{1,2}, Wei Li^{1,2} and Lingxia Yang^{1,2}

¹School of Petrochemical Engineering, Lanzhou University of Technology, China

²Machinery Industry Pump Special Valve Engineering Research Center, China

³Manufacturing Company of China National Logging Corporation, China

Submitted: March 26, 2026; Published: April 10, 2026

*Corresponding author: Huaxing Zhai, Manufacturing Company of China National Logging Corporation, Xi'an, Shaanxi 710201, China

Abstract

High-pressure hydrogen (70MPa) pressure reduction systems are critical in fields such as fuel cell drones, yet the extreme pressure drop and complex dynamic behavior present challenges to conventional design approaches, including low efficiency and difficulties in handling nonlinear control. This paper designs and refines a compact two stage pressure reducing valve that achieves both smooth pressure reduction and ease of manufacturability. To address the performance prediction challenge, dynamic maximum tree depth technology and tree-based gene expression programming (Tree GEP) is introduced to optimize the kernel function of Gaussian process regression (GPR), resulting in a high precision dynamic performance prediction model. Subsequently, by incorporating chaotic mapping and dynamic inertia weights to enhance the whale optimization algorithm (WOA), a chaotic dynamic multi objective optimization framework (CDMOWOA) is established for the global optimization of the valve's structural parameters. The results demonstrate that after optimization, the steady state outlet pressure is reduced by 4.08 %, the overshoot is lowered by 11.79 %, and the dynamic response time is shortened by 14.4%. While maintaining a stable output of 0.3 MPa, a synergistic improvement in both response speed and control accuracy is realized. The research outcomes provide theoretical support and an efficient toolset for the intelligent design and performance evolution studies of key components in hydrogen energy propulsion systems.

Keywords: Two-stage hydrogen Pressure reducing valve; Dynamic performance prediction; Machine learning surrogate model; Elastic net; multi-objective optimization

Abbreviations: GPR: Gaussian process regression; WOA: whale optimization algorithm; UAVs: unmanned aerial vehicles; UAVs: unmanned aerial vehicles; ML: machine learning; GPR: Gaussian process regression; SVM: Support Vector; ANN: Machines Artificial Neural Networks; RSM: Response Surface Methodology; GA: Genetic Algorithm; PSO: Particle Swarm Optimization; OLHD: Optimal Latin Hypercube Design; OLHS: Optimal Latin Hypercube Sampling; GPR: Gaussian Process Regression; CPK: Composite Kernels; GEP: Gene Expression Programming; GP: Genetic Programming; Tree-GEP: Tree-based Gene Expression Programming; BIC: Bayesian Information Criterion; RMSE: Root Mean Square Error

Introduction

As the core power source for hydrogen-powered unmanned aerial vehicles (UAVs), the performance of the fuel cell system directly determines the overall operational effectiveness of the UAV. The hydrogen pressure reducing valve, serving as a critical control component within the fuel cell system, has the primary function of progressively reducing the pressure of hydrogen from high-pressure storage tanks to the specific range required by the fuel cell stack. This process provides a stable flow of low-pressure gas to the down-stream pneumatic circuit. With the

increasing demand for UAVs and heightened requirements for endurance performance, hydrogen-powered UAVs impose more stringent performance demands on high-pressure hydrogen reducing valves. Single-stage pressure reducing valves struggle to simultaneously meet the requirements of a large pressure reduction ratio and high control accuracy under high-pressure operating conditions. In contrast, two-stage hydrogen pressure reducing valves achieve precise regulation from high pressure to the working pressure through a two-stage pressure reduction

structure. Within this configuration, the first-stage valve bears the main responsibility for pressure reduction, while the second-stage valve is tasked with the precise control of the output pressure. However, when the inlet pressure reaches levels as high as 70MPa, the pressure reduction effectiveness of the first-stage valve often proves unsatisfactory. This inadequacy leads to insufficient control precision in the output pressure of the second-stage valve, thereby seriously compromising the safety and stability of the hydrogen fuel cell system.

Consequently, research and development focused on the design of high-pressure hydro-gen valves for fuel cells hold significant theoretical and engineering importance. Further-more, the dynamic performance of hydrogen pressure reducing valves is notably influenced by multi-physics coupling effects and complex operating conditions. Traditional modeling approaches, which rely on empirical formulas or finite element simulations, struggle to accurately capture their dynamic characteristics. Structural optimization is of-ten dependent on numerous high-cost, long-cycle trial-and-error experiments, lacking a solid theoretical foundation for optimization. Therefore, identifying research methodologies capable of rapidly and accurately obtaining the dynamic performance of two-stage hydrogen pressure reducing valves and achieving efficient structural optimization is of paramount importance.

In recent years, machine learning (ML) technology has provided new avenues for performance prediction and optimization of complex systems, leveraging its powerful nonlinear modeling capabilities and adaptive learning characteristics for high-dimensional data [1]. By extracting complex nonlinear relationships from vast amounts of data, ML can accurately predict the dynamic response characteristics of systems. With the rapid development of data-driven methods and ML techniques, researchers have applied ML to the study of dynamic performance prediction for mechanical components [2-5,6] established a Gaussian process regression (GPR) prediction model based on a combined kernel function. The model was validated using different Gaussian regression methods, and the results demonstrated that the combined kernel function-based regression model possesses high prediction accuracy for both steady-state and transient operating conditions. [7], based on a “combined prediction” approach, integrated a grey model with RCF neural network weights to establish a performance pre-diction model for a centrifugal compressor. [8] constructed a regression prediction model and conducted a comprehensive study on predicting the dynamic characteristics of design parameters using ML and deep learning techniques, evaluating the dynamic characteristics of the housing. [9] built a performance prediction model for a cycle gasoline engine based on Support Vector Machines (SVM), importing control parameters obtained during the optimization

process as inputs to predict the engine’s performance output. In summary, ML methods have been widely applied in performance pre-diction for pumps, valves, impellers, and engines. However, research on two-stage hydrogen pressure reducing valves still predominantly relies on traditional mechanism model-based prediction methods, and no scholar has yet applied ML methods to predict their dynamic response performance. Therefore, constructing a high-precision dynamic performance prediction model for the two-stage hydrogen pressure reducing valve based on ML methods provides a new technical pathway for enhancing the design efficiency and performance optimization of hydrogen pressure reducing valves, holding significant theoretical importance and engineering value.

Traditional optimization methods, which typically focus on a single performance metric, offer advantages of model simplicity and high solution efficiency. However, they often struggle to capture the multi-dimensional requirements inherent in engineering problems. In the optimal design of fluid machinery such as pumps, valves, and compressors, design objectives frequently involve multiple conflicting performance indicators. Consequently, multi-objective optimization has become an indispensable technique in the optimization of precision components like gas pressure reducing valves [10-12] utilized Artificial Neural Networks (ANN) and Response Surface Methodology (RSM) to establish performance prediction models, and then employed a Genetic Algorithm (GA) to perform both single-objective and multi-objective optimization of key structural parameters, obtaining the Pareto front for density and absolute pressure drop ratio. [13] adopted a novel non-dominated sorting and chaotic mutation multi-objective gravitational search algorithm to establish a multi-objective optimization model. They selected suitable solutions using an improved entropy weight method and a relative target closeness method for a comprehensive comparative study of basic parameters. [14] proposed a hierarchical optimization algorithm composed of an Elite Non-dominated Sorting Genetic Algorithm (NSGA-II) and a multi-objective Particle Swarm Optimization (PSO) algorithm based on r-dominance. This multi-objective PSO algorithm employed r-dominance to replace traditional Pareto dominance for structural optimization and improvement. [15] introduced enhanced Lévy flight and adaptive learning factors into the Chicken Swarm Optimization (CSO) algorithm, pro-posing a hybrid algorithm combining a Genetic Algorithm and an improved CSO. Simultaneously, they developed and validated a prediction model based on a phenomenological approach, and optimized a marine engine using this combined optimization algorithm. In summary, multi-objective optimization methods, implemented through various algorithms, have been widely applied by scholars in the optimal design of fluid machinery. However, no scholar has yet applied multi-objective optimization methods to the structural

parameter optimization of two-stage hydrogen pressure reducing valves. Coupling surrogate models with an improved Whale Optimization Algorithm for the multi-objective optimization of the structural parameters of the two-stage hydrogen pressure reducing valve can effectively enhance the safety and stability of the fuel cell hydrogen supply system.

This paper presents a two-stage hydrogen pressure reducing valve characterized by its compact structure, rapid response, and high control accuracy, and conducts simulation studies on its dynamic characteristics and control precision. By integrating artificial intelligence methods with swarm intelligence optimization algorithms, and utilizing the structural parameters of the two-stage hydrogen pressure reducing valve as inputs with the outlet pressure steady-state value, overshoot, and dynamic response time as dynamic performance evaluation indicators, a high-precision and efficient dynamic performance prediction model and a structural parameter optimization model for the two-stage hydrogen pressure reducing valve are constructed. This framework enables the rapid and accurate acquisition of the valve's dynamic performance and the identification of optimal structural parameters that meet performance requirements, thereby effectively enhancing performance computation efficiency and structural optimization speed. Consequently, the experimental cycle is shortened, and testing costs are reduced. This study provides a valuable reference for the structural design and performance prediction of two-stage hydro-gen pressure reducing valves and offers certain guidance for the design of self-operated valves.

The main contributions of this study are summarized as follows.

- i. A dynamic performance prediction framework for a two-stage hydrogen pressure reducing valve is established by integrating Optimal Latin Hypercube Sampling (OLHS) with a coupled surrogate modeling strategy. The proposed framework improves the efficiency of structural parameter exploration within a high-dimensional design space.
- ii. An Elastic Net-based feature selection method is introduced to identify the key structural parameters affecting the dynamic performance of the valve. This approach effectively reduces feature redundancy and improves the robustness of the surrogate model.
- iii. A multi-objective optimization model for the structural parameters of the two-stage hydrogen pressure reducing valve is constructed based on the DTGP-CK-GPR surrogate model and the CDMOWOA algorithm, enabling the coordinated optimization of multiple dynamic performance indicators.

Structural Design of the Two-Stage Hydrogen Pressure Reducing Valve and Establishment of the System Dynamics Model

The operational architecture of the hydrogen pressure regulation system employs a cascading two-stage configuration, as illustrated in Figure 1, comprising sequentially arranged primary and secondary pressure reducing valves. The primary valve assembly integrates essential components including a main spring, piston, auxiliary spring, valve core, and valve seat. A distinctive tapered configuration is adopted for the primary valve core, engineered to generate substantial flow resistance and sustain significant pressure differentials, thereby ensuring operational stability throughout the pressure reduction sequence. The dual-spring mechanism operates through coordinated action: the main spring modulates core displacement in response to hydraulic forces to regulate valve opening, while the complementary auxiliary spring provides stabilizing assistance in maintaining precise core positioning.

The secondary regulation stage incorporates a diaphragm-based assembly consisting of main and auxiliary springs, valve core, and seat components. The secondary valve core utilizes a planar geometry that minimizes flow resistance while offering manufacturing advantages through simplified fabrication requirements. Furthermore, the system integrates an intelligent pressure feedback mechanism where decompressed hydrogen is channeled through a dedicated feedback orifice into a pressure monitoring chamber. When output pressure exceeds the designated 0.3MPa threshold, the accumulated gas actuates the diaphragm to recalibrate the valve core position, achieving pressure equilibrium and providing critical overpressure protection.

The two-stage hydrogen pressure reducing valve consists of two direct-acting pressure reducing units arranged in series, where the first-stage valve undertakes the bulk of pressure reduction while the second-stage valve ensures precise output pressure regulation. Leveraging the valve's architectural configuration, pressure-reduction methodology, and internal flow characteristics, we developed a system dynamics simulation model using MATLAB/Simulink to investigate its dynamic operational characteristics. In the simulation model, hydrogen is treated as a compressible ideal gas, and the thermodynamic behavior within each chamber is described through pressure-temperature state equations. Mechanical friction and leakage effects are incorporated in simplified forms to capture their influence on the valve dynamics. Under maintained operational conditions of 70MPa inlet pressure and 0.3MPa outlet pressure, the research systematically examines how varying structural parameters influence the valve's dynamic behavior and pressure regulation precision.

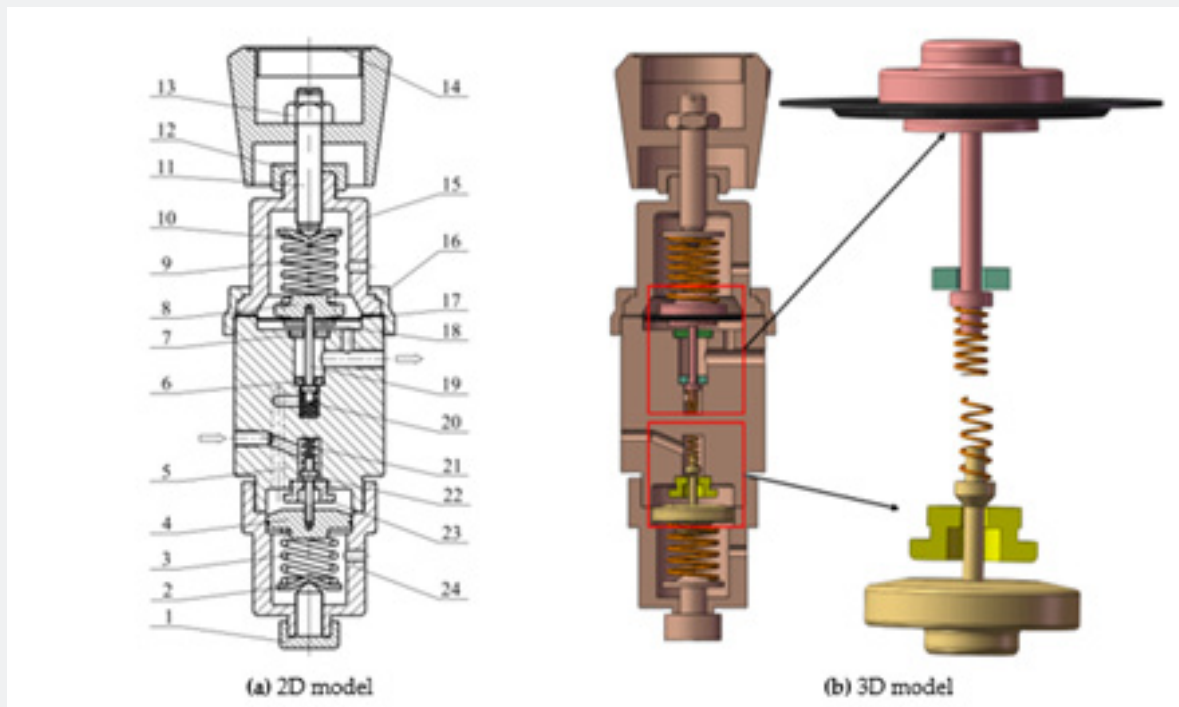


Figure 1: Structural model of the two-stage hydrogen pressure reducing valve.

1. Lower adjustment bolt 2. Lower regulating shim 3. Main spring of first-stage valve 4. Piston 5. Valve body 6. Valve seat of second-stage valve 7. Sealing gasket of second-stage valve 8. Sealing disk 9. Main spring of second-stage valve 10. Upper regulating shim 11. Upper adjustment bolt 12. Knob handle 13. Valve stem nut 14. Knob handle cover 15. Upper valve cap 16. Fastening clamp ring 17. Diaphragm 18. Spring washer 19. Valve core of second-stage valve 20. Auxiliary spring of second-stage valve 21. Auxiliary spring of first-stage valve 22. Valve core of first-stage valve 23. Valve seat of first-stage valve 24. Lower valve cap.

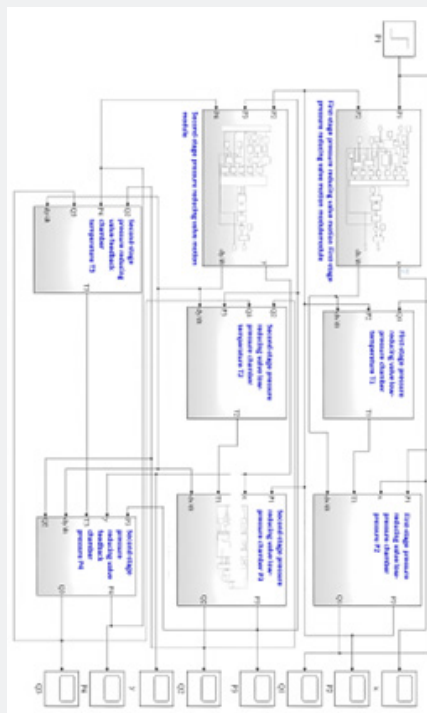


Figure 2: System dynamic characteristics simulation model.

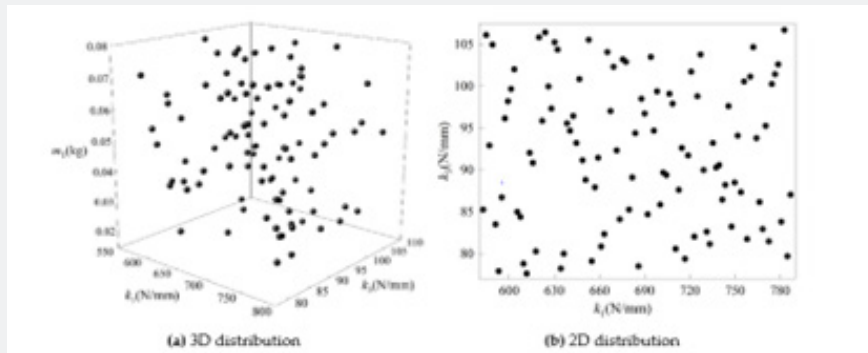


Figure 3: Distribution of experimental design sample points extracted by the OLHS method.

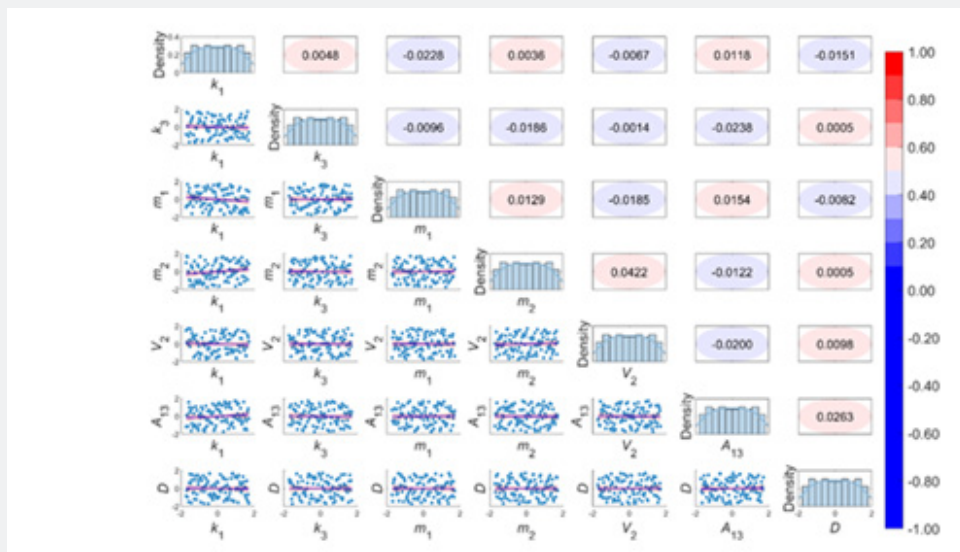


Figure 4: Correlation coefficients among the features.

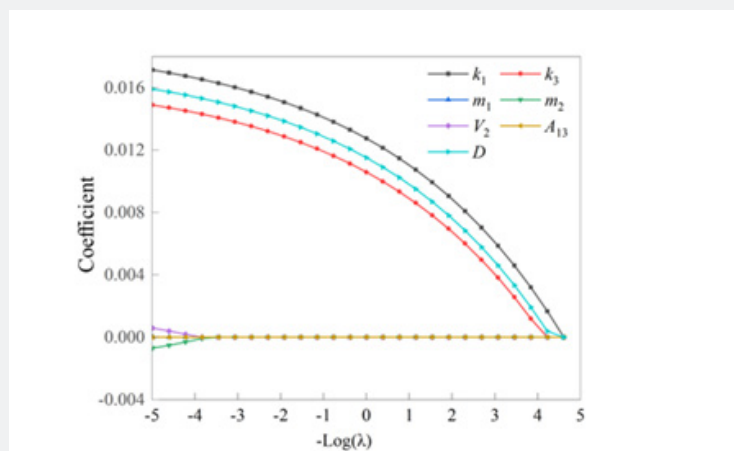


Figure 5: Feature selection results for the steady-state outlet pressure.

After encapsulating sub-modules using the Subsystem or S-function blocks in MATLAB/Simulink, the dynamic characteristic simulation model of the two-stage hydro-gen pressure reduction valve system was established by connecting the input and output ports of each sub-module with signal lines. The dynamic characteristic simulation model of the two-stage hydrogen pressure reduction valve system is shown in Figure 2. Through modular design, the complex system dynamic equations are decomposed into multiple functionally independent sub-modules, improving simulation flexibility and scalability. The simulation module of the two-stage hydrogen pressure reduction valve system mainly consists of three sub-modules: the valve core motion component sub-module, the chamber pressure differential equation sub-module, and the chamber thermodynamic equation sub-module.

The valve core motion component sub-module is divided into the first-stage pressure reduction valve core motion component module and the second-stage pressure reduction valve motion component module. The first-stage pressure reduction valve core motion component module takes the system inlet pressure P_1 and the first-stage pressure reduction valve outlet pressure P_2 as inputs, and outputs the displacement x , velocity v_1 , and acceleration a_1 of the first-stage valve core motion component. The second-stage pressure reduction valve motion component module takes the second-stage pressure reduction valve inlet pressure P_2 , system outlet pressure P_3 , and second-stage pressure reduction valve feedback chamber pressure P_4 as inputs, and outputs the displacement y , velocity v_2 , and acceleration a_2 of the second-stage valve core motion component.

The chamber pressure differential equation sub-module is divided into the first-stage low-pressure chamber pressure module, the second-stage low-pressure chamber pressure module, and the second-stage pressure reduction valve feedback chamber pressure module. These modules primarily take the inlet pressure of each chamber, the displacement of the valve core motion component, the velocity of the valve core motion component, and the temperature of each chamber as inputs, and output the outlet pressure of each chamber and the mass flow rate at each valve port of the pressure reduction valve.

The chamber thermodynamic equation sub-module is divided into the first-stage low-pressure chamber temperature module, the second-stage low-pressure chamber temperature module, and the second-stage pressure reduction valve feedback chamber temperature module. These modules mainly take the outlet pressure of each chamber, the mass flow rate at each valve port of the pressure reduction valve, and the velocity of the valve core motion component as inputs, and output the temperature

of each chamber. The detailed governing equations of the valve dynamics have been reported in our previous study [16]. The key fixed parameters used in the simulation model are summarized in Appendix A.

In this study, the working medium (hydrogen) is treated as an ideal gas to simplify the dynamic modeling of the pressure reducing valve. The detailed modeling assumptions and justification for the ideal gas approximation under high-pressure conditions have been discussed in our previous work [16]. Although real gas effects and the Joule-Thomson effect may become noticeable at pressures approaching 70MPa, the ideal gas assumption provides a reasonable approximation for capturing the dynamic response characteristics of the valve system. The potential influence of real gas behavior mainly affects thermodynamic accuracy but has limited impact on the structural parameter optimization and dynamic trend analysis performed in this work.

The MATLAB/Simulink dynamic model used in this study is based on a previously validated framework reported in [16]. Although detailed validation results are not repeated here to avoid redundancy and maintain conciseness, the model structure, governing equations, and parameter settings remain consistent with the validated framework. Key dynamic responses such as outlet pressure overshoot and response time fall within the ranges reported in prior studies, ensuring the reliability of the simulated data used for machine learning prediction and multi-objective optimization.

Establishment of the Dynamic Performance Prediction Model Data-base and Data Processing

Construction of the sample database

Prior to constructing the dynamic performance prediction model for the two-stage hydrogen pressure reducing valve, it is essential to define the model's inputs and outputs. The various structural parameters of the two-stage hydrogen pressure reducing valve are designated as the input variables for the prediction model, while the dynamic performance indicators serve as the output variables. To ensure solutions remain within the feasible domain and to avoid non-physical results, the design variables must be reasonably constrained. Excessively large variable values may lead to system instability or overshoot exceeding limits, whereas excessively small values could impair the system response speed. Consequently, the final determined constraint ranges for the design variables are listed in Table 1.

The database serves as a critical factor influencing the prediction accuracy of the model, making the establishment of a comprehensive and valid database essential. Optimal Latin Hypercube Design (OLHD) represents a stratified Monte

Carlo sampling methodology that enhances the uniformity of conventional Latin Hypercube Design through spatial filling and balancing strategies [17]. In scenarios with limited sample sizes, OLHD demonstrates the capability to efficiently acquire test samples with superior performance characteristics while maintaining reasonable computational resource utilization. In

this study, the OLHD method was employed to extract 100 sample points. The corresponding steady-state outlet pressure (P_w), overshoot (δ), and dynamic response time (T_s) for each sample point were computed utilizing the simulation model developed in Chapter 2. A partial representation of the resulting sample database is presented in Table 2.

Table 1: Constraint Ranges of Design Variables.

Design Variable	Characteristic Variable	Lower Limit	Upper Limit
First-stage main spring stiffness k_1 (N/mm)	x_1	582.7	786.9
Second-stage main spring stiffness k_3 (N/mm)	x_2	77.65	106.72
First-stage valve core mass m_1 (kg)	x_3	0.02	0.08
Second-stage valve core mass m_2 (kg)	x_4	0.01	0.13
First-stage low-pressure chamber volume V_2 (mm ³)	x_5	7234.56	10449.92
Second-stage feedback orifice area A_{13} (mm ²)	x_6	10.05	13.82
Second-stage diaphragm outer diameter D (mm)	x_7	30	45

Table 2: Partial Sample Database of Structural Parameters.

k_1	k_3	m_1	m_2	V_2	A_{13}	D	P_w	δ	T_s
x_1	x_2	x_3	x_4	x_5	x_6	x_7	y_1	y_2	y_3
681.71	89.1	0.04	0.12	8046.52	12.83	32.58	0.2977	0.2457	0.4122
758.02	81.76	0.07	0.11	7981.56	11.88	40.61	0.3109	0.271	0.4305
741.52	86.46	0.04	0.06	9832.83	13.82	43.03	0.3172	0.2074	0.5199
599.2	98.2	0.06	0.09	9183.26	10.13	30.45	0.2941	0.2448	0.3732
...		
642.52	96.44	0.04	0.09	8631.13	10.09	36.06	0.3038	0.2086	0.4387
636.33	80	0.02	0.02	8793.52	12.79	38.03	0.2962	0.2182	0.5013
628.08	97.32	0.05	0.13	7754.21	11.76	42.88	0.3084	0.193	0.3881
706.46	99.09	0.02	0.06	9508.05	11.38	31.21	0.3082	0.1965	0.5237

Figure 3 illustrates the distribution of experimental design sample points generated using the OLHS method. As observed in the figure, both training and testing sample points are evenly distributed throughout the parameter space without exhibiting significant clustering phenomena. This demonstrates excellent space-filling properties, effectively preventing issues of sparsity or overcrowding in local regions, thereby providing high-quality data support for model training.

Normalization processing

Prior to constructing the machine learning model, preprocessing was performed on the obtained experimental data to accelerate the convergence of the training process and improve prediction accuracy. Normalization is a procedure that reorganizes data in the database to meet two fundamental requirements [18].

It maps the minimum and maximum values of each input variable in the dataset to 0 and 1, respectively, while proportionally scaling all other values between them to the range [0,1]. As the input variables in the sample library exhibit comparable orders of magnitude, they were mapped to the interval [0,1] according to Equation (1).

$$X_{normalize} = \frac{x - x_{min}}{x_{max} - x_{min}} \in [0,1] \tag{1}$$

Where $X_{normalize}$ represents the normalized value; x_{max} denotes the maximum value; x_{min} indicates the minimum value; and x corresponds to the original value. The sample database after normalization of input variables is presented in Table 3.

Table 3: Partial Sample Database of Structural Parameters after Normalization of Input Variables.

k_1	k_3	m_1	m_2	V_2	A_{13}	D	P_w	δ	T_s
x_1	x_2	x_3	x_4	x_5	x_6	x_7	y_1	y_2	y_3
0.485	0.394	0.384	0.929	0.253	0.737	0.172	0.2977	0.2457	0.4122
0.859	0.141	0.889	0.818	0.232	0.485	0.707	0.3109	0.271	0.4305
0.778	0.303	0.283	0.444	0.808	1	0.869	0.3172	0.2074	0.5199
0.081	0.707	0.636	0.707	0.606	0.02	0.03	0.3172	0.2074	0.5199
...
0.293	0.646	0.364	0.647	0.434	0.01	0.404	0.3038	0.2086	0.4387
0.263	0.081	0.061	0.061	0.485	0.727	0.535	0.2962	0.2182	0.5013
0.222	0.677	0.455	0.99	0.162	0.455	0.859	0.3084	0.193	0.3881
0.606	0.738	0.01	0.434	0.707	0.354	0.081	0.3082	0.1965	0.5237

The normalized dataset was randomly partitioned into two subsets, with 70% of the data allocated to the training set and the remaining 30% designated as the test set. The training set was utilized to train the proposed prediction model for forecasting the dynamic performance of the two-stage hydrogen pressure reducing valve, while the test set served to validate the model's performance by evaluating its generalization capability and prediction accuracy in predicting the valve's dynamic characteristics.

Although only 100 Optimal Latin Hypercube Sampling (OLHS) sampling points were generated, Latin Hypercube Design ensures uniform coverage of the seven-dimensional feature space, which mitigates potential sampling bias. In addition, the predictive performance of the model was evaluated on an independent test dataset using RMSE and R² metrics to assess its generalization capability. Feature selection via Elastic Net further reduces model complexity and enhances model robustness.

Feature Selection Based on Elastic Net

In the performance prediction study of the two-stage hydrogen pressure reducing valve, the specific roles of individual feature variables in the prediction process remain unclear, potentially leading to interference from redundant features and issues of model complexity during model construction. Therefore, a feature selection method based on Elastic Net is employed to screen the feature variables, eliminating redundant or irrelevant features and retaining key variables that significantly contribute to the model's predictive performance, which subsequently serve as input variables for the prediction model.

Elastic Net combines Lasso regression (*L1* regularization) and Ridge regression (*L2* regularization), enabling automatic variable selection and continuous shrinkage to enhance prediction accuracy while effectively avoiding overfitting [19]. Specifically,

Elastic Net performs feature selection by combining *L1* and *L2* regularization penalties, which shrink regression coefficients and automatically eliminate less important variables. The expression for the Elastic Net model is given by:

$$f_w(x) = \arg \min_{\omega} \left\{ \frac{1}{N} \sum_{i=1}^N (y_i - X(x^i; \omega))^2 + \lambda_1 \|\omega\|_2 + \lambda_2 \|\omega\|_1 \right\} \quad (2)$$

Where y_i represents different dynamic response indicators, X denotes the matrix composed of different structural parameters; ω represents the least squares coefficients; λ_1 and λ_2 are the regularization coefficients for Lasso regression and Ridge regression, respectively. The regularization parameters λ_1 and λ_2 were set according to [1] to balance model sparsity and prediction accuracy.

During the feature selection process, the Pearson correlation coefficient method was initially employed to analyze the correlations among the structural parameters of the two-stage hydrogen pressure reducing valve. Preliminary screening was conducted by calculating the linear correlation coefficients between pairs of variables. As shown in Figure 4, which presents the correlation coefficients among various features, a larger absolute value of the correlation coefficient indicates a stronger correlation. It can be observed that the maximum absolute value of the correlation coefficients among all features of the two-stage hydrogen pressure reducing valve is 0.0422, which is significantly less than 1. Consequently, there are no strong correlations between the various features of the valve, indicating that the structural parameters are independent of each other. This makes them suitable as input variables for the prediction model, thereby avoiding the negative impact of multicollinearity on model performance.

Although the pairwise correlations among features are small, Elastic Net is still employed to enhance model robustness and interpretability by automatically identifying and removing less important or noisy variables. This approach helps prevent overfitting, simplifies the surrogate model, and highlights the key structural parameters that most significantly influence the valve's dynamic performance.

The Elastic Net method was employed to assess the contribution values of individual features to the dynamic performance indicators. This technique performs feature selection through fitting and regularization processes, where the absolute magnitude of the coefficients indicates the degree of contribution of each feature to the objective function. Specifically, larger absolute values signify greater feature importance, while features with coefficients equal to zero are considered non-influential.

Figure 5 presents the feature selection results for the steady-state outlet pressure. The first-stage main spring stiffness, second-stage main spring stiffness, and second-stage diaphragm outer diameter demonstrate the highest importance for the steady-state outlet pressure of the two-stage hydrogen pressure reducing valve, with corresponding absolute feature coefficients of 0.0186, 0.0163, and 0.0174, respectively. These parameters show positive correlations with the steady-state outlet pressure. The absolute feature coefficients of all other features remain below 0.001, indicating their negligible influence.

Figure 6 shows the feature selection results for the outlet pressure overshoot. The first-stage valve core mass, second-stage main spring stiffness, and second-stage diaphragm outer diameter demonstrate the highest importance for the outlet pressure overshoot of the two-stage hydrogen pressure reducing valve, with corresponding absolute feature coefficients of 0.0636, 0.0755, and 0.0541, respectively. The first-stage valve core mass shows a positive correlation with the overshoot, while the second-stage main spring stiffness and second-stage diaphragm outer diameter exhibit negative correlations with the overshoot.

Figure 7 presents the feature selection results for the outlet pressure dynamic response time. The first-stage main spring stiffness, first-stage valve core mass, and second-stage valve core mass demonstrate the highest importance for the dynamic response time of the two-stage hydrogen pressure reducing valve, with corresponding absolute feature coefficients of 0.1478, 0.1262, and 0.1028, respectively. The first-stage main spring stiffness shows a positive correlation with the dynamic response time, whereas the first-stage and second-stage valve core masses exhibit negative correlations with the dynamic response time.

Based on the comprehensive Elastic Net feature selection results, five key variables demonstrating significant contributions

to the model's predictive performance were identified: k_1 , k_3 , m_1 , m_2 , and D . These screened independent variables will serve as the input parameters for the dynamic performance prediction model of the two-stage hydrogen pressure reducing valve.

To further interpret the statistical results obtained from the Elastic Net model, the physical mechanisms associated with the key parameters are analyzed from the perspective of valve dynamics and gas compressibility.

The first-stage main spring stiffness (k_1) directly influences the dynamic balance between the spring restoring force and the inlet pressure acting on the valve core. A higher stiffness increases the restoring force, which accelerates the valve closing process but may also introduce stronger dynamic oscillations in the pressure regulation process. Consequently, variations in k_1 can significantly affect the response speed and stability of the outlet pressure.

The second-stage main spring stiffness (k_3) plays a crucial role in the secondary decompression process. In high-pressure hydrogen systems, the gas inside the decompression chamber exhibits strong compressibility, which forms a coupled feedback mechanism between the spring force and gas expansion. Changes in k_3 modify the equilibrium between these forces, thereby influencing pressure fluctuation characteristics and outlet pressure overshoot.

In addition, the valve core masses (m_1 and m_2) affect the inertia of the valve motion. Larger valve core masses increase the dynamic inertia of the system, which can delay the response of the pressure regulation process while potentially suppressing rapid oscillations under certain operating conditions.

Therefore, the feature importance results obtained from the Elastic Net model are consistent with the physical mechanisms governing the dynamic behavior of the two-stage hydrogen pressure reducing valve.

It should be noted that the feature selection process in this study aims to identify the dominant structural parameters that significantly influence the dynamic performance indicators of the two-stage hydrogen pressure reducing valve. The statistical relationships revealed by the Elastic Net method do not imply complete physical independence among structural parameters. In practical engineering systems, parameters such as spring stiffness, valve core mass, and diaphragm dimensions may exhibit inherent coupling relationships that jointly influence the dynamic response of the valve. These interaction effects are implicitly considered in the subsequent multi-objective optimization process, where multiple structural parameters are simultaneously optimized through the CDMOWOA algorithm to determine the optimal parameter combination.

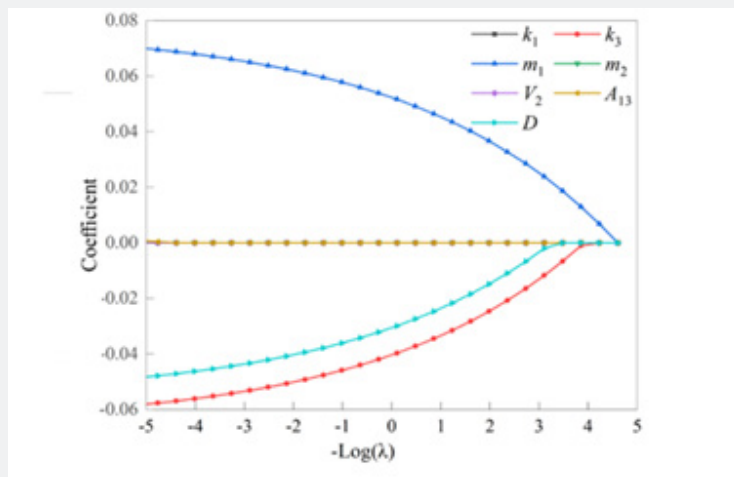


Figure 6: Feature selection results for the overshoot.

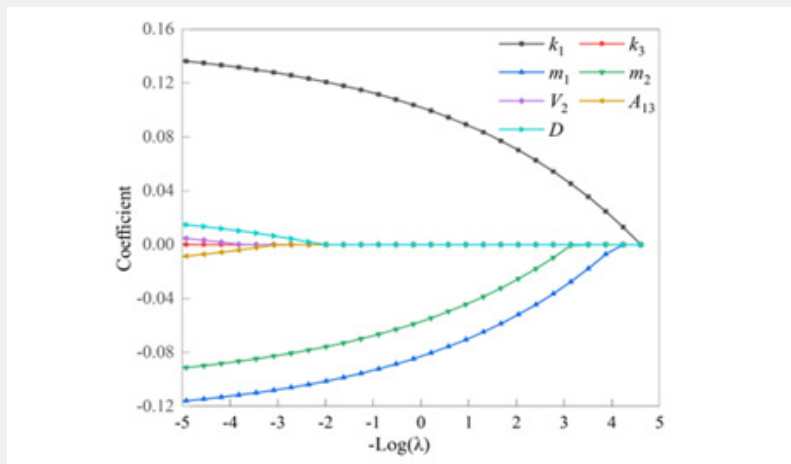


Figure 7: Feature selection results for the outlet pressure dynamic response time.

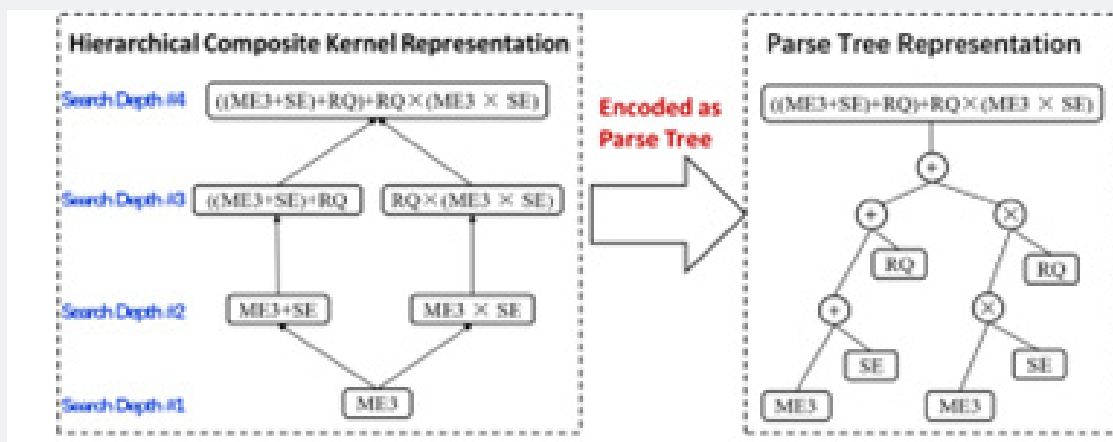


Figure 8: Structure diagram of the encoded CPK.

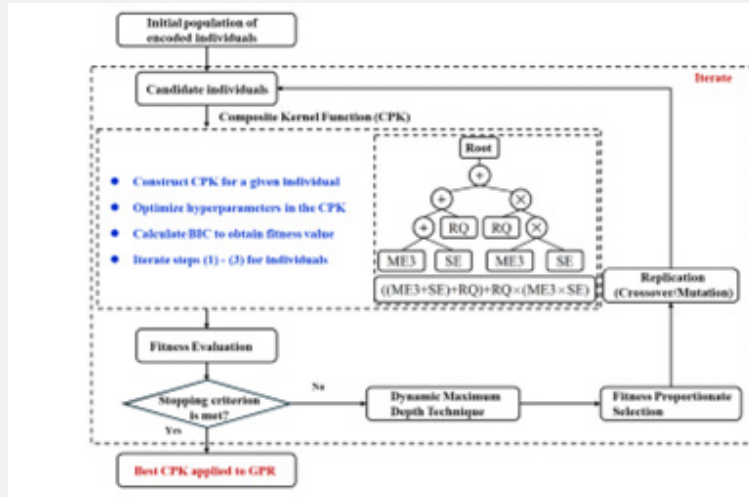


Figure 9: Flowchart of Gaussian Process Regression with composite kernel function based on dynamic tree structure.

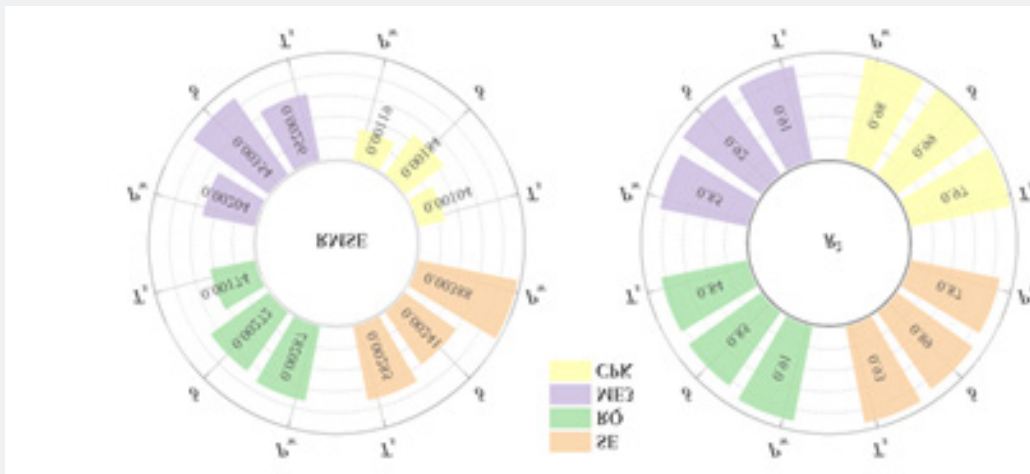


Figure 10: Comparison of predictive performance for different kernel functions..

Dynamic Performance Prediction of the Two-Stage Hydrogen Pressure Reducing Valve

Construction of the dynamic performance prediction model

Gaussian Process Regression (GPR) is a machine learning technique grounded in statistical learning theory and Bayesian theory, making it suitable for handling complex nonlinear relationships [20]. The predictive performance of GPR is highly dependent on the covariance function (kernel). However, current research predominantly determines the covariance function empirically, which can compromise the prediction accuracy of GPR models. [21] proposed tree-based genetic programming for GPR, which encodes Composite Kernels (CPK) as tree structures and utilizes tree-based genetic programming to discover the optimal tree structure for the composite kernel. Building

upon this method, the present study incorporates a dynamic maximum tree depth technique [22] to establish a Gaussian Process Regression model with composite kernel learning based on dynamic tree depth genetic programming (DTGP-CK-GPR), thereby effectively mitigating the issue of excessive complexity in genetic programming solutions.

Gene Expression Programming (GEP) represents a fusion and innovation of concepts from Genetic Algorithms (GA) and Genetic Programming (GP). By introducing a genotype/phenotype separation mechanism, it significantly extends and surpasses the capabilities of traditional genetic algorithms. GEP is employed to automatically construct programs or to discover optimal structures for nonlinear input-output models. Its expression can be represented as:

$$\hat{y}(k) = \sum_{i=1}^{n_a} f_i [y(k-i)] + \sum_{j=1}^{n_b} g_j [u(k-j)] + e(k) \quad (3)$$

Where f_i and g_j are nonlinear scalar functions; $e(k)$ denotes the modeling error; n_a and n_b represent the orders of the input and output, respectively.

Tree-based Gene Expression Programming (Tree-GEP) encodes individuals within a population into parse tree representations through genetic operations such as crossover and mutation. In order to allow the Composite Kernel (CPK) to learn more flexible structures, a hierarchical composite kernel is integrated and encoded using Tree-GEP. The resulting encoded CPK structure is illustrated in Figure 8.

In each generation of Tree-GEP, all individuals are evaluated using a fitness function to assess the quality of potential solutions. Tree-GEP generates offspring from parents based on genetic operations to enhance the population's average fitness value. After an individual is generated, the Bayesian Information Criterion (BIC) is employed as the fitness function within Tree-GEP, penalizing overly complex solutions by favoring a better marginal likelihood. The Bayesian Information Criterion is expressed as:

$$BIC(M) = -2 \log p(D|M) + p \log N \quad (4)$$

where $p(D|M)$ denotes the optimized marginal likelihood of the training data (D); N and p represent the number of training data points and the hyperparameters in the kernel, respectively.

The search space for parse trees may be infinite. During the evolutionary process, the depth and size of a parse tree may increase without a corresponding improvement in fitness value. To prevent excessive growth of parse trees, a dynamic maximum tree depth technique is introduced to adjust the depth limit. When new individuals are generated in offspring through crossover or mutation, their acceptance and the applicable depth limit are determined based on their fitness values. The expression for the dynamic maximum tree depth technique is:

$$Best_f = \begin{cases} \min(Best_f, f(i)) & d(i) \leq Max_d \\ f(i) & d(i) > Max_d, f(i) < Best_f \end{cases} \quad (5)$$

Where $Nind$ is the total number of individuals; d is the depth of each individual; f is the fitness of each individual; $Best_f$ is the best fitness; and Max_d is the depth limit.

During the evolutionary process, the best individual appearing in any generation is selected as the optimal structure for the CPK

until the stopping criteria are met. The flowchart of the proposed Gaussian Process Regression with composite kernel function based on the dynamic tree structure is shown in Figure 9.

RMSE and R^2 were adopted as metrics to compare the errors between the training predicted values and the original dataset under different conditions. The expressions for each metric are as follows:

Root Mean Square Error (RMSE):

$$RMSE = \sqrt{\frac{1}{N} \sum_{i=1}^N (\hat{y}_i - y_i)^2} \quad (6)$$

Coefficient of Determination (R^2):

$$R^2 = 1 - \frac{\sum_{i=1}^N (y_i - \hat{y}_i)^2}{\sum_{i=1}^N (y_i - \bar{y}_i)^2} \quad (7)$$

where y_i represents the true value, \hat{y}_i denotes the predicted value of the true value, \bar{y}_i is the mean of the true values, and N is the number of samples.

The DTGP-CK-GPR model was implemented in a Python programming environment. Three commonly used kernel functions and the proposed composite kernel function were selected for training and prediction to forecast different dynamic performance indicators. The evaluation metrics of the results from different kernel functions are presented in Figure 10. When predicting dynamic performance indicators using different kernel functions, the composite kernel function (CPK) achieved the lowest Root Mean Square Error (RMSE) and the highest Coefficient of Determination (R^2) closest to 1. This indicates that the proposed composite kernel function possesses the best fitting performance and is more effective in predicting the dynamic performance of the two-stage hydrogen pressure reducing valve.

After validating the predictive performance of the proposed composite kernel function (CPK), a Gaussian process regression prediction model based on the dynamic tree-structured composite kernel was constructed. The maximum depth of the dynamic tree was set to 10, the reproduction rate in the genetic programming was set to 0.1, and the probabilities of crossover and mutation were both set to 0.5 to ensure an equal likelihood of generating offspring. The constructed Gaussian process regression prediction model was then used to predict the test dataset, and the prediction results are shown in Figure 11.

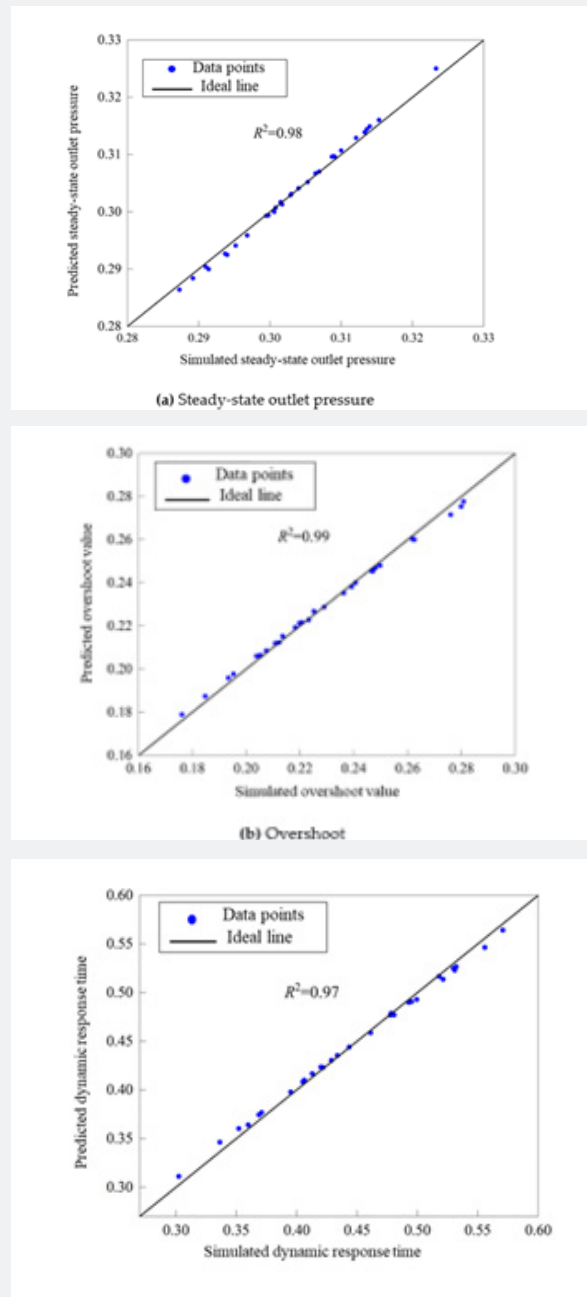


Figure 11: Correlation between simulated and predicted values for the test set.

As shown in Figure 11, the predicted results for the test set yield coefficients of determination R^2 of 0.99, 0.97, and 0.98 for overshoot, dynamic response time, and steady-state value, respectively. The data points align closely with the ideal line. Although a minimal number of points deviate due to the presence of generalization error, their influence on the overall prediction is negligible. A high degree of correlation is observed between the simulated and predicted values. This strong correlation demonstrates that the constructed Gaussian process regression prediction model, based on the dynamic tree-structured composite kernel function, exhibits excellent fitting performance on the test

set. The model achieves high prediction accuracy on the test data, possesses strong generalization capability, and is therefore suitable for predicting the dynamic performance of the two-stage hydrogen pressure reducing valve.

Analysis of dynamic performance prediction results

The trained DTGP-CK-GPR prediction model was employed to forecast the dynamic performance of the two-stage hydrogen pressure reducing valve, with the prediction results presented in Figure 12-14.

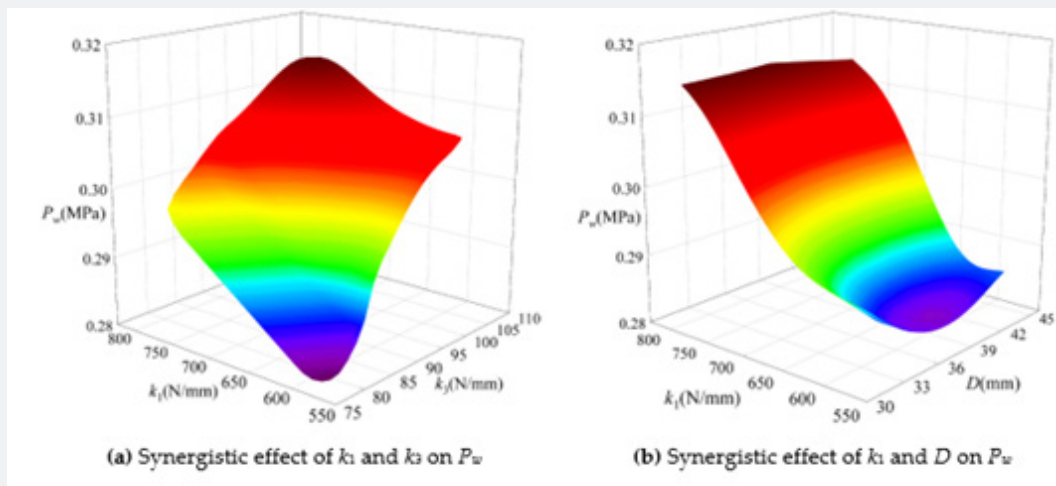


Figure 12: Predicted distribution of the system's steady-state outlet pressure.

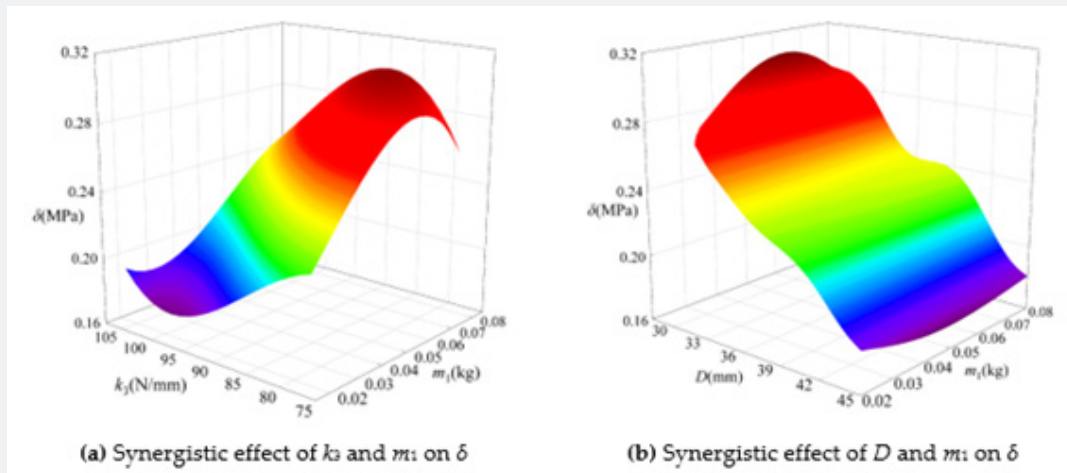


Figure 13: Predicted distribution of the system overshoot.

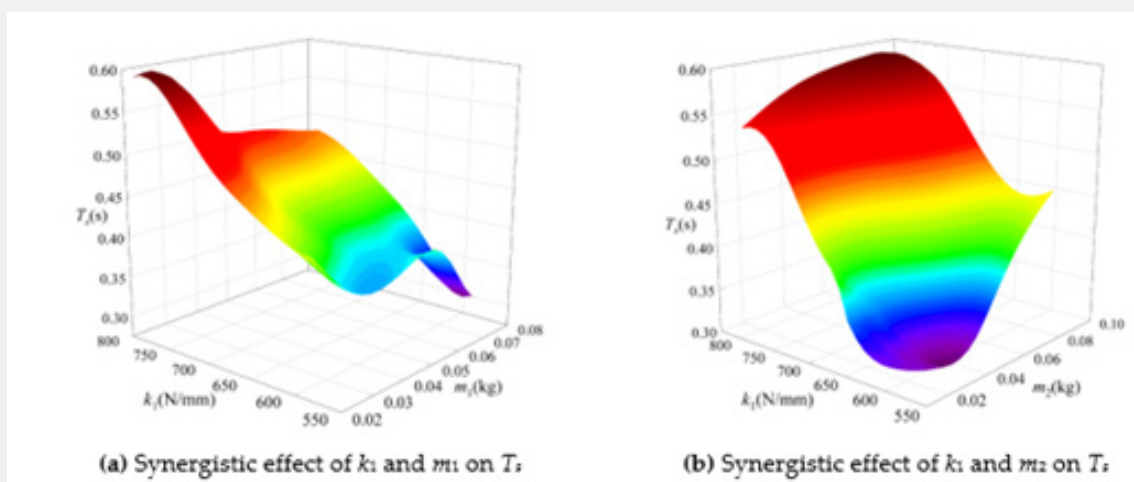


Figure 14: Predicted distribution of the system dynamic response time.

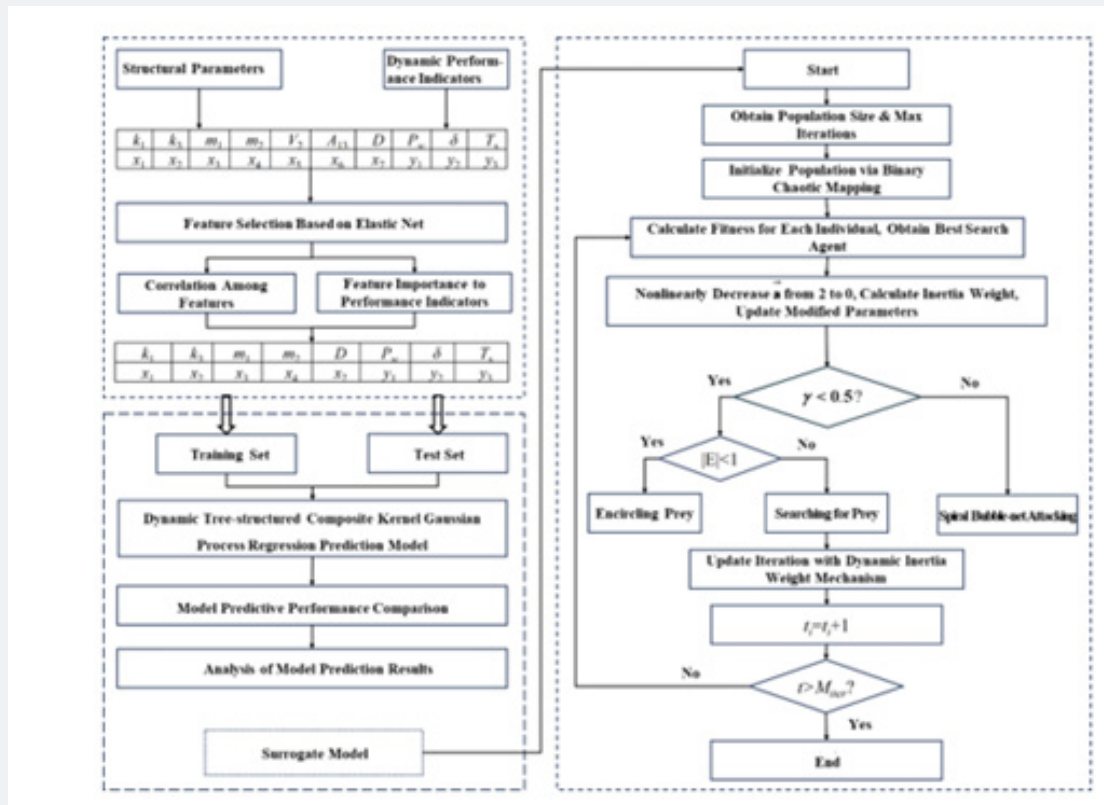


Figure 8: Structure diagram of the encoded CPK.

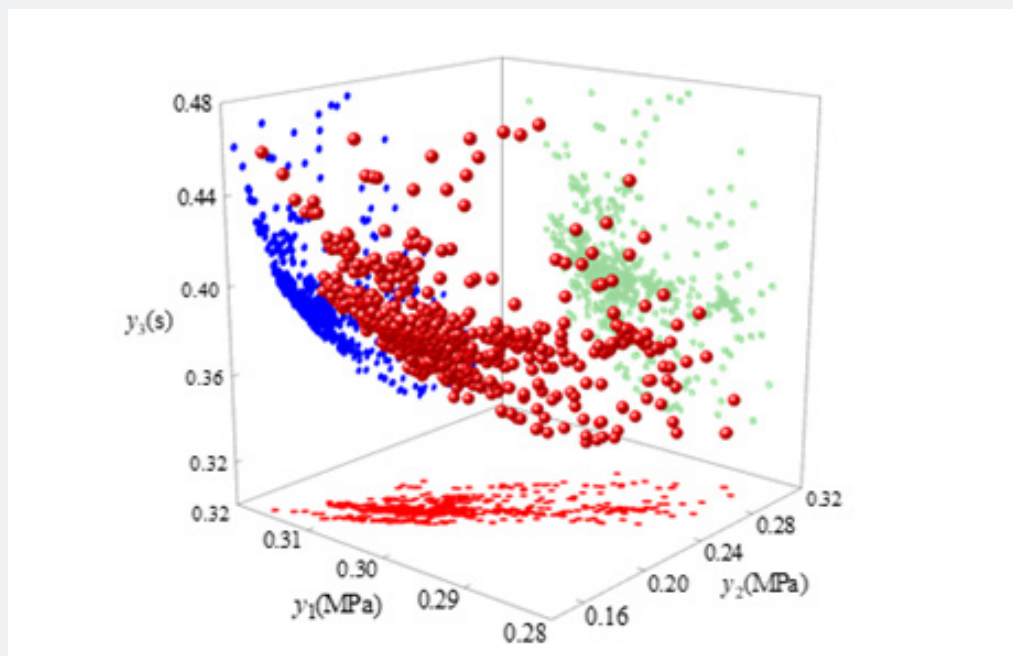


Figure 16: Pareto front solutions of the optimization model based on the CDMOWOA.

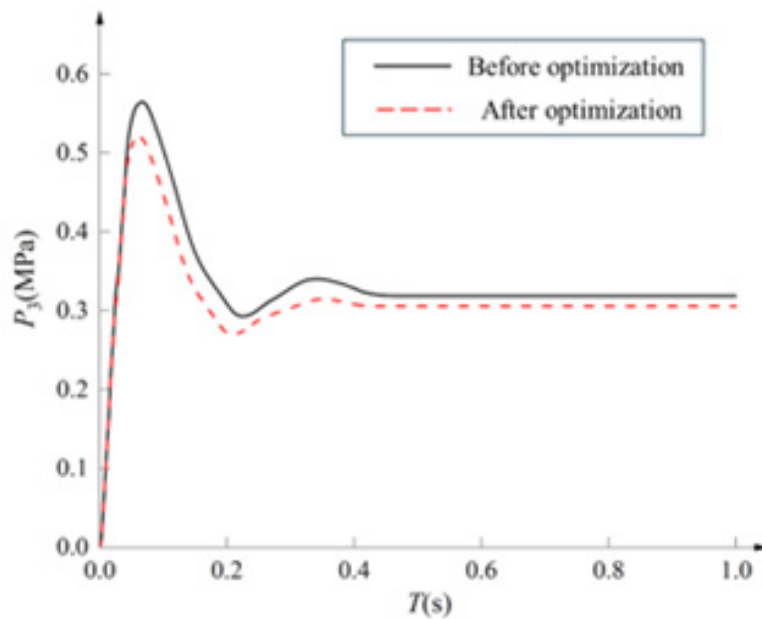


Figure 17: Dynamic characteristic curves of the two-stage hydrogen pressure reducing valve before and after optimization.

Figure 12(a) illustrates the influence of the first-stage main spring stiffness (k_1) and the second-stage main spring stiffness (k_2) on the system's steady-state outlet pressure. As shown, the steady-state outlet pressure gradually increases with rising values of both k_1 and k_2 . The trend of the response surface becomes progressively steeper, indicating a significantly enhanced synergistic effect on the steady-state outlet pressure.

Figure 12(b) depicts the impact of the first-stage main spring stiffness (k_1) and the second-stage diaphragm outer diameter (D) on the steady-state outlet pressure. The synergistic effect surface exhibits a characteristic steep slope. As both k_1 and D increase, the synergistic effect strengthens markedly, with the maximum steady-state outlet pressure reaching 0.316 MPa. Therefore, the rational design of the first-stage main spring stiffness, second stage main spring stiffness, and second-stage diaphragm outer diameter can effectively enhance the pressure control accuracy of the system.

Figure 13(a) presents the influence of the second-stage main spring stiffness (k_2) and the first-stage valve core mass (m_1) on the system outlet pressure overshoot. The figure shows that as the second-stage main spring stiffness k_2 decreases and the first-stage valve core mass m_1 increases, the overshoot of the system outlet pressure rises rapidly. The maximum overshoot reaches 0.312MPa, indicating a significantly enhanced synergistic effect on the outlet pressure overshoot.

Figure 13(b) illustrates the effect of the second-stage main spring stiffness (k_2) and the second-stage diaphragm outer diameter (D) on the outlet pressure overshoot. It can be observed that the diaphragm outer diameter has a more pronounced influence on the over-shoot compared to changes in the first-stage valve core mass. This suggests that the diaphragm outer diameter exerts a more significant effect on the overshoot than the first-stage valve core mass. Furthermore, the synergistic effect surface exhibits a steep slope characteristic. As the second-stage diaphragm outer diameter decreases and the first-stage valve core mass increases, the synergistic surface becomes steeper, leading to a more substantial impact on the overshoot.

Figure 14(a) illustrates the influence of the first-stage main spring stiffness (k_1) and the first-stage valve core mass (m_1) on the dynamic response time (T_s) of the system outlet pressure. As can be seen from the figure, k_1 and m_1 demonstrate a significant synergistic effect on T_s , and they exert opposing effects on T_s . As the first-stage main spring stiffness decreases and the first-stage valve core mass increases, the outlet pressure reaches its steady-state value more rapidly.

Figure 14(b) shows the impact of the first-stage main spring stiffness (k_1) and the second stage valve core mass (m_2) on the dynamic response time of the system outlet pressure. It can be observed that the synergistic effect surface of k_1 and m_2 on the dynamic response time exhibits a characteristic steep slope,

indicating a clear interactive effect. During the design process, the values of the first-stage main spring stiffness and the second stage valve core mass should be comprehensively considered to enable the system to achieve the steady-state value faster and shorten the dynamic response time.

Multi-objective Optimization of Structural Parameters for the Two-Stage Hydrogen Pressure Reducing Valve Based on a Coupled Surrogate Model

Construction of the multi-objective optimization model for structural parameters

Before conducting the optimization of the structural parameters for the two-stage hydrogen pressure reducing valve, it is imperative to define the value ranges of the design variables and select the optimization objectives. The steady-state outlet pressure, over-shoot, and dynamic response time serve as the primary dynamic evaluation indicators. Among these, the steady-state outlet pressure reflects the control accuracy of the pressure reducing valve, while the overshoot and dynamic response time indicate its regulation performance and stability.

Based on the analysis in Chapter 5, the first-stage main spring stiffness, the second stage main spring stiffness, and the second-stage diaphragm outer diameter have the greatest influence on the steady-state outlet pressure of the two-stage hydrogen pressure reducing valve. The first-stage valve core mass, the second-stage main spring stiffness, and the second-stage diaphragm outer diameter exert the most significant impact on the outlet pressure overshoot. Furthermore, the first-stage main spring stiffness, the first-stage valve core mass, and the second-stage valve core mass are the dominant factors affecting the dynamic response time of the outlet pressure. It is not feasible to enhance either the control accuracy or the regulation performance of the valve by altering a single structural parameter, nor is it possible to determine the optimal structural parameters through isolated adjustments.

The first-stage main spring stiffness k_1 , second-stage main spring stiffness k_2 , second stage diaphragm outer diameter D , first-stage valve core mass m_1 , and second-stage valve core mass m_2 , which have the greatest impact on the system's outlet performance, are selected as the optimization variables. The dynamic performance indicators steady state outlet pressure P_w , overshoot δ , and dynamic response time T_s are designated as the optimization objectives. Within the defined ranges of the optimization variables, the Chaotic Dynamic Whale Optimization Algorithm is employed to optimize the structural parameters of the two-stage hydrogen pressure reducing valve, aiming to determine the optimal parameter set. Based on these optimization variables and objectives, the objective function and constraints are formulated. Considering machining tolerances and installation

allowances, the value ranges of the optimization variables and the objective function are defined as follows:

$$\begin{aligned} \min Y &= [y_2, y_3] = [\delta, T_s] \\ \text{Subject to } & |P_w - 0.3\text{MPa}| \leq 0.01\text{MPa} \\ & \begin{cases} 582.7 \leq k_1 \leq 786.9\text{N/mm} \\ 77.65 \leq k_2 \leq 106.72\text{N/mm} \\ 0.02 \leq m_1 \leq 0.08\text{kg} \\ 0.01 \leq m_2 \leq 0.13\text{kg} \\ 30 \leq D \leq 45\text{mm} \end{cases} \end{aligned} \quad (8)$$

The multi-objective optimization aims to minimize the outlet pressure overshoot δ and the dynamic response time T_s , while ensuring that the steady-state outlet pressure P_w remains close to the design target of 0.3MPa. The constraint on P_w is expressed as $|P_w - 0.3| \leq 0.01\text{MPa}$, reflecting engineering requirements for pressure regulation accuracy. The variable bounds are determined based on mechanical design limits, machining tolerances, and installation allowances. This formulation ensures that the optimization results are physically meaningful and practically implementable.

The trade-offs between overshoot and response time are considered from the perspective of actuator limits, system stability, and control performance. For example, increasing the first-stage main spring stiffness k_1 can reduce response time but may increase over-shoot, while adjusting valve core masses m_1 and m_2 can reduce overshoot without significantly affecting the steady-state pressure. This coupling ensures that the final solution represents a balanced engineering trade-off.

To address the issue of the Whale Optimization Algorithm (WOA) being prone to converging to local optima, the Chaotic Dynamic Multi-objective Whale Optimization Algorithm (CDMOWOA) employs nonlinear parameters to replace linear ones throughout both the exploration and exploitation phases of WOA. This modification aims to accelerate convergence, improve accuracy, and refine the spiral update position. Additionally, a dynamic inertia weight coefficient is introduced to balance the exploration and exploitation phases, further enhancing the convergence rate.

i. Chaotic mapping population initialization

In chaos theory, the irregularity and disorder of dynamic systems are governed by deterministic laws, which can help enhance the convergence speed of optimization problems. To increase the diversity of the search space, the Tent chaotic map and the Circle chaotic map are combined during the initialization phase [23]. The expression for the combined chaotic mapping is:

$$B = \begin{bmatrix} b_{11} & b_{12} & \cdots & b_{1,N} \\ b_{21} & b_{12} & \cdots & b_{2,N} \\ \vdots & \vdots & \ddots & \vdots \\ b_{M1} & b_{M2} & \cdots & b_{M,N} \end{bmatrix} \quad (9)$$

$$f(b_{j,n}) = \begin{cases} f_i(a, b_{j,n}) & 0 < H \leq 0.5 \\ f_c(c, d, b_{j,n}) & 0.5 < H \leq 1 \end{cases} \quad (10)$$

$$b_{j+1,n} = f(b_{j,n}) \times \gamma(b_{j,n}) \quad (11)$$

$$\vec{B}_i = \vec{B}_{lb} + (\vec{B}_{ub} - \vec{B}_{lb}) \vec{b} \quad (12)$$

Where B represents the population initialization; b denotes the boundary; M is the population size; N is the number of variables; $\gamma(b)$ is a linear mapping used to transfer the variable range from $[0,1]$ to the specified value range; and H is a random number between 0 and 1.

The Tent chaotic map can be expressed as:

$$f_i(a, b_j) = b_{j+1} = \begin{cases} b_j & b_j < 0.7 \\ 0.7 & \\ 1 - b_j & b_j > 0.7 \\ 0.3 & \end{cases} \quad (13)$$

The Circle chaotic map can be expressed as:

$$f_c(c, d, b_n) = b_j + 1 = \text{mod} \left(b_j + d - \frac{c}{2\pi} \sin(2\pi b_j), 1 \right) \quad (14)$$

Where b_j is the current state at time step j ; b_{j+1} is the next state at time step $j+1$; the chaotic vector; where D is the dimension of the search space.

ii. Convergence factor

In the WOA algorithm, the convergence factor used in the exploration and exploitation phases decreases linearly from 2 to 0. CDMOWOA replaces the original linear convergence factor with a nonlinear one, expressed as:

$$\vec{a} = 2 + 2 \cdot \cos \left[\frac{\pi}{2} \times \left(1 + \frac{t}{M_{iter}} \right) \right] \quad (15)$$

Where $Miter$ is the maximum number of iterations.

iii. Dynamic inertia weight coefficient

In the standard WOA, the inertia weight is typically fixed at 1, which can make the algorithm prone to becoming trapped in local minima. [24] defined the inertia weight value as ω and updated it throughout the iterative process to achieve better convergence. Its expression is:

$$\omega = \left| \cos \left(\frac{et\pi}{M_{iter}} \right) \right| \quad (16)$$

where ω denotes the adaptive inertia weight function; e represents a value that decreases from 1 to 0; and t indicates the current iteration. The new update mechanism is defined as:

$$\vec{x}(t+1) = \begin{cases} \omega \vec{X}^*(t) - \vec{E} \cdot \vec{C} \cdot \vec{X}^*(t) - \vec{X}(t) & q < 0.5 \\ \left[\vec{X}^*(t) - \vec{X}(t) \right] \cdot e^{bl} \cdot \cos(2\pi l) + \omega \vec{X}^*(t) & q \geq 0.5 \end{cases} \quad (17)$$

$$\vec{X}(t+1) = \omega \vec{X}_{rand}(t) - \vec{E} \cdot \vec{H} \quad (18)$$

The dynamic performance prediction model for the two-stage hydrogen pressure reducing valve established in Chapter 5 was utilized as the surrogate model. The Chaotic Dynamic Multi-objective Whale Optimization Algorithm (CDMOWOA) was then employed to construct the optimization framework for refining the structural parameters and identifying the optimal parameter combination. This resulted in a multi-objective optimization model coupled with the surrogate model, as illustrated in Figure 15.

Analysis of optimization results for the structural parameters of the two-stage hydrogen pressure reducing valve

The dynamic performance prediction model for the two-stage hydrogen pressure reducing valve, developed in Chapter 5, was employed as the surrogate model. Coupled with the Chaotic Dynamic Multi-objective Whale Optimization Algorithm, this setup was used to perform the structural parameter optimization. The initial population size for the optimization model was set to 30, and the number of iterations was set to 100.

It should be noted that the optimization variables are constrained within the same parameter ranges used for constructing the surrogate model in Chapter 5. Therefore, the optimization process is conducted within the valid prediction domain of the surrogate model, ensuring the reliability of the surrogate-based optimization results.

Through computation, the Pareto front solutions obtained

from the optimization model based on the CDMOWOA are presented in Figure 16. As shown in Figure 16, the optimization results illustrate the trade-offs between overshoot and dynamic response time under the outlet pressure constraint. Three distinct schemes emerge: one corresponding to the minimum overshoot, another to the shortest dynamic response time, and a third where the outlet pressure most closely approaches the design specifications. By comprehensively considering both the dynamic response performance and the stability of the two-stage hydrogen pressure reducing valve, the optimal combination of structural parameters was determined.

The CDMOWOA optimization model was employed to solve for the optimal structural parameter combination. These optimal parameters were subsequently simulated using the Simulink dynamic characteristics model. The results before and after optimization are presented in Table 4 and Figure 17. As shown,

the optimal structural parameters for the two-stage hydrogen pressure reducing valve obtained by the CDMOWOA optimization model coupled with the surrogate model are as follows: first-stage main spring stiffness of 668.2N/mm, second-stage main spring stiffness of 98.7N/mm, first-stage valve core mass of 0.052 kg, second-stage valve core mass of 0.047kg, and second-stage diaphragm outer diameter of 45mm. Following optimization, the steady-state outlet pressure of the valve decreased by 4.08%, bringing it closer to the design specification. Additionally, the overshoot was reduced by 11.79%, and the dynamic response time decreased by 14.4%. These results demonstrate a significant improvement in the dynamic performance of the two-stage hydrogen pressure reducing valve. Compared to the initial parameters, the CDMOWOA optimization model successfully identified the optimal structural parameter set, improved the efficiency of the optimization process, and effectively enhanced the stability of the system outlet pressure.

Table 4: Solution Results Based on the CDMOWOA Model.

Solution	Structural Parameters					Target Values		
	k_1 (N/mm)	k_2 (N/mm)	m_1 (kg)	m_2 (kg)	D (mm)	P_w (MPa)	δ (MPa)	T_s (s)
Initial Optimized	647.4	92.5	0.06	0.05	40	0.319	0.246	0.403
	668.2	98.7	0.052	0.047	45	0.306	0.217	0.345

The optimization process simultaneously considers the coupled influence of multiple structural parameters, which implicitly accounts for the interaction effects among parameters in practical engineering systems.

According to Figure 17, compared with the preliminary design of the two-stage hydro-gen pressure reducing valve, the Chaotic Dynamic Multi-objective Whale Optimization Algorithm (CDMOWOA) coupled with the surrogate model significantly enhances the dynamic response performance of the valve. This improvement contributes to greater stability in the hydrogen supply system for the fuel cell of the hydrogen-powered unmanned aerial vehicle. The results demonstrate that the proposed high-efficiency multi-objective optimization model can be effectively applied to the structural parameter optimization of the two-stage hydrogen pressure reducing valve.

It should be noted that the selected optimal solution reflects the coupled effects of the key structural parameters. For example, increasing the first-stage main spring stiffness k_1 improves stability but may increase dynamic response time, while adjusting

the valve core masses m_1 and m_2 can reduce overshoot but slightly affect steady-state outlet pressure. Similarly, the second-stage diaphragm diameter D influences both pressure regulation and system compliance. The final optimized combination represents a balanced trade-off among these interdependent parameters, achieving significant overshoot reduction, faster response, and closer adherence to the design outlet pressure. This explanation highlights the physical interactions between parameters and the rationale for selecting the optimal solution from the Pareto front.

It should be noted that the post-optimization simulations using the Simulink dynamic model mainly verify the consistency between the optimization results and the system dynamic model. Since the surrogate model was constructed based on simulated data, these simulations cannot be considered as fully independent validation. Nevertheless, they confirm that the optimized parameter set improves the dynamic performance within the modeling framework adopted in this study.

From an engineering perspective, the dynamic characteristics of the pressure reducing valve are closely related to the operational

safety of the hydrogen supply system operating at high pressure levels up to 70MPa. Excessive outlet pressure overshoot may temporarily exceed the allowable pressure limits of downstream components, potentially triggering overpressure protection mechanisms or causing structural stress to the fuel cell supply system. Therefore, reducing overshoot is important for preventing transient over-pressure risks.

Similarly, the dynamic response time affects the stability of the pressure regulation process. Slow response may lead to delayed pressure regulation under rapidly changing load conditions, while overly aggressive regulation may induce oscillations or instability in the pressure control system. By reducing both overshoot and response time, the optimized structural parameters improve the pressure regulation stability and reduce the potential operational risks associated with high-pressure hydrogen supply systems.

Therefore, the selected optimization objectives are not only related to dynamic performance but also contribute to improving the safety and reliability of the hydrogen pressure regulation process in practical engineering applications. These safety and operational risk considerations follow insights from recent studies [25,26].

Conclusion

To address issues such as the narrow pressure regulation range and insufficient output pressure control accuracy of existing gas pressure reducing valves, a compact, fast-response, and high-precision high-pressure-difference two-stage hydrogen pressure reducing valve has been designed. An integrated approach combining numerical simulation and artificial intelligence was employed to construct a high-precision and efficient dynamic response performance prediction model and a structural parameter optimization model for the two-stage hydrogen pressure reducing valve. The main research conclusions are as follows:

i. Building upon the system dynamics simulation model developed in Matlab/Simulink, a high-precision dynamic performance prediction model (DTGP-CK-GPR) for the two-stage hydrogen pressure reducing valve was proposed by improving the Gaussian Process Regression model through the introduction of tree-based genetic programming and a dynamic maximum tree depth technique. The Elastic Net feature selection method was used to screen the feature variables. Preprocessed data were divided into training and testing sets to train and validate the high-precision prediction model. In the test dataset, the coefficients of determination (R^2) for the outlet pressure overshoot, dynamic response time, and steady-state value were 0.99, 0.97, and 0.98,

respectively, with corresponding root mean square errors (RMSE) of 0.0020, 0.0051, and 0.0008. These results demonstrate that the DTGP-CK-GPR model possesses excellent fit-ting performance and significantly improves the efficiency of performance prediction.

ii. By coupling the Chaotic Dynamic Multi-objective Whale Optimization Algorithm (CDMOWOA) with the DTGP-CK-GPR model, the structural parameters of the two-stage hydrogen pressure reducing valve were optimized. The optimal structural parameters obtained are as follows: first-stage main spring stiffness of 668.2N/mm, second-stage main spring stiffness of 98.7 N/mm, first-stage valve core mass of 0.052 kg, second-stage valve core mass of 0.047 kg, and second-stage diaphragm outer diameter of 45mm. After optimization, the steady-state outlet pressure decreased by 4.08%, the overshoot was reduced by 11.79%, and the dynamic response time was shortened by 14.4%. The resulting outlet pressure meets the design specifications, proving that this multi-objective optimization model coupled with a surrogate can be effectively applied to the optimization of structural parameters for two-stage hydrogen pressure reducing valves.

Future Work

Future work will focus on experimental validation using a physical prototype of the two-stage hydrogen pressure reducing valve to further verify the effectiveness of the optimized structural parameters under real operating conditions.

Author Contributions

Conceptualization, S.L. and Y.Z.; methodology, Y.Z.; software, Y.Z.; validation, Y.Z. and W.L.; formal analysis, Y.Z.; investigation, H.Z.; resources, S.L.; data curation, Y.Z.; writing—original draft preparation, H.Z.; writing—review and editing, W.L. and L.Y.; visualization, H.Z.; supervision, S.L. and L.Y.; project administration, S.L.; funding acquisition, S.L. All authors have read and agreed to the published version of the manuscript.

Funding

This research was funded by the National Natural Science Foundation of China (Research Project: 51569012), the Double First-Class Key Program of Gansu Provincial Department of Education; Gansu Province Science and Technology Program (Grant No. 22CX8GA125) and Gansu Provincial Department of Education (Industrial Support Plan Project: 2025CYZC-048).

Data Availability Statement

The original contributions presented in the study are included in the article, further inquiries can be directed to the corresponding author.

Table A1: Simulation parameters used in the dynamic model.

Parameter	Symbol	Value	Source
Hydrogen gas constant	R	4124 J/(kg·K)	literature
Heat capacity ratio	ν	1.41	literature
Specific heat at constant pressure	C_p	14300 J/(kg·K)	literature
Discharge coefficient	C_d	0.62	valve handbook
Valve spool mass	m	design value	valve design
Spring stiffness	k	design value	design specification
Damping coefficient	c	empirical value	engineering estimate
Initial gas temperature	T_0	300K	operating condition

References

- Li H, Xu B, Lu G, Du C, Huang N (2021) Multi-objective optimization of PEM fuel cell by coupled significant variables recognition, surrogate models and a multi-objective genetic algorithm. *Energy Conversion and Management* 236.
- Han M, Liu Y, Zheng K, Ding Y, Wu D (2020) Investigation on the modeling and dynamic characteristics of a fast-response and large-flow water hydraulic proportional cartridge valve. *Proceedings of the Institution of Mechanical Engineers. Part C: Journal of Mechanical Engineering Science* 234(22): 4415-4432.
- Chen X, Pan P, Wang T (2023) Nonlinear Dynamic Characteristics Analysis of Planar Mechanism Multibody System Considering Lubrication Clearances. *International Journal of Precision Engineering and Manufacturing* 24: 2033-2055.
- Hou J, Li S, Pan W, Yang L (2023) Co-Simulation Modeling and Multi-Objective Optimization of Dynamic Characteristics of Flow Balancing Valve. *Machines* 11(3): 337.
- Mi J, Huang G (2023) Dynamic Prediction of Performance Degradation Characteristics of Direct-Drive Electro-Hydraulic Servo Valves. *Applied Sciences* 13(12): 7231.
- Shi X, Jiang D, Qian W, Liang Y (2022) Application of the Gaussian Process Regression Method Based on a Combined Kernel Function in Engine Performance Prediction. *ACS Omega* 7(45): 41732-41743.
- Peng Q, Bao R, Li J, Ren J, Tang J, et al. (2024) Centrifugal compressor performance prediction and dynamic simulation of natural gas hydrogen blended. *International Journal of Hydrogen Energy* 52: 872-893.
- Lee W, Jung TY, Lee S (2023) Dynamic Characteristics Prediction Model for Diesel Engine Valve Train Design Parameters Based on Deep Learning. *Electronics* 12(8): 1806.
- Tong J, Li Y, Liu J, Cheng R, Guan J, et al. (2021) Experiment analysis and computational optimization of the Atkinson cycle gasoline engine through NSGA-II algorithm using machine learning. *Energy Conversion and Management* 238: 113871.
- Yang M, Zhang Y, Ai C, Yan G, Jiang W (2023) Multi-objective optimization of K-shape notch multi-way spool valve using CFD analysis, discharge area parameter model, and NSGA-II algorithm. *Engineering Applications of Computational Fluid Mechanics* 17(1): 2242721.
- Chen FQ, Zhang Y, Jin ZJ (2023) Co-design and aerodynamic study on a two-step high pressure reducing system for hydrogen decompression: From hydrogen refueling station to hydrogen fuel cell vehicle. *International Journal of Hydrogen Energy* 48: 10968-10981.
- Kou C, Alghassab MA, Abed AM, Alkhalaf S, Alharbi FS, et al. (2024) Modeling of hydrogen flow decompression from a storage by a two-stage Tesla valve: A hybrid approach of artificial neural network, response surface methodology, and genetic algorithm optimization. *Journal of Energy Storage* 85: 111104.
- Zhang T, Zhou J, Yang X, Li H (2022) Multi-objective optimization and decision-making of the combined control law of guide vane and pressure regulating valve for hydroelectric unit. *Energy Science & Engineering* 10(2): 472-487.
- Liu L, Guo Y (2020) Multi-objective optimization for attitude maneuver of liquid-filled flexible spacecraft based on improved hierarchical optimization algorithm. *Applied Soft Computing* 96: 106598.
- Chen X, Liu L, Du J, Liu D, Huang L, et al. (2022) Intelligent Optimization Based on a Virtual Marine Diesel Engine Using GA-ICSO Hybrid Algorithm. *Machines* 10(4): 227.
- Zhai H, Li S, Zhang Y, Li W, Yang L (2026) Dynamic Simulation and Characteristic Analysis of a Two-Stage Hydrogen Pressure-Reducing Valve. *Designs* 10(2): 27.
- Liu D, Wang S, Shi J, Liu D (2024) GA based construction of maximin Latin hypercube designs for uncertainty design of experiment with dynamic strategy management. *Applied Soft Computing* 167: 112454.
- Garg R, Bhargava A (2024) Bug prediction based on deep neural network with reptile search optimization to enhance software reliability. *Multimedia Tools and Applications* 83: 75869-75891.
- Severson KA, Attia PM, Jin N, Perkins N, Jiang B, et al. (2019) Data-driven prediction of battery cycle life before capacity degradation. *Nature Energy* 4: 383-391.
- Schulz E, Speekenbrink M, Krause A (2018) A tutorial on Gaussian process regression: Modelling, exploring, and exploiting functions. *Journal of Mathematical Psychology* 85: 1-16.
- Roman I, Santana R, Mendiburu A, Lozano JA (2021) Evolving Gaussian process kernels from elementary mathematical expressions for time series extrapolation. *Neurocomputing* 462: 426-439.
- Jin SS (2020) Compositional kernel learning using tree-based genetic programming for Gaussian process regression. *Structural and Multidisciplinary Optimization* 62: 1313-1351.
- Elmogly A, Miquirish H, Elawady W, El-Ghaish H (2023) ANWOA: an adaptive nonlinear whale optimization algorithm for high-dimensional optimization problems. *Neural Computing and Applications* 35: 22671-22686.
- Sun G, Shang Y, Yuan K, Gao H (2022) An Improved Whale Optimization Algorithm Based on Nonlinear Parameters and Feedback Mechanism. *International Journal of Computational Intelligence Systems* 15(38).

25. Lu Y, Cao X, Wang Z, Xu S, Sun S (2026) A review of metal dust explosion characteristics and protection technologies. Journal of Safety and Sustainability.
26. Stemn E, Martey IM, Fosu S (2025) Descriptive and bowtie analysis of commercial fire outbreaks in Ghana: Threats, consequences and control measures. Journal of Safety and Sustainability 2(4): 293-306.



This work is licensed under Creative Commons Attribution 4.0 License
DOI: [10.19080/JOJMS.2026.10.555790](https://doi.org/10.19080/JOJMS.2026.10.555790)

**Your next submission with JuniperPublishers
will reach you the below assets**

- Quality Editorial service
- Swift Peer Review
- Reprints availability
- E-prints Service
- Manuscript Podcast for convenient understanding
- Global attainment for your research
- Manuscript accessibility in different formats
(Pdf, E-pub, Full Text, Audio)
- Unceasing customer service

Track the below URL for one-step submission

<https://juniperpublishers.com/submit-manuscript.php>